

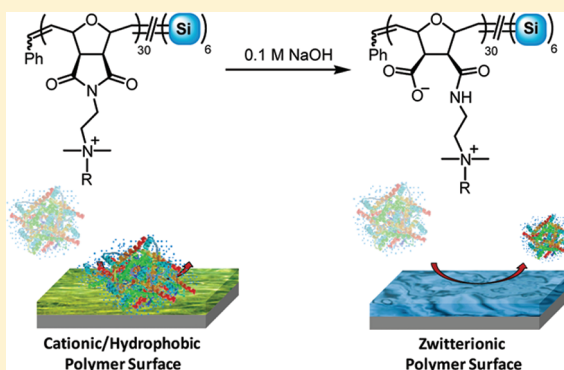
Dual-Functional ROMP-Based Betaines: Effect of Hydrophilicity and Backbone Structure on Nonfouling Properties

Semra Colak and Gregory N. Tew*

Department of Polymer Science and Engineering, University of Massachusetts—Amherst, Conte Research Center for Polymers, 120 Governor's Drive, Amherst, Massachusetts 01003, United States

Supporting Information

ABSTRACT: Foundational materials for nonfouling coatings were designed and synthesized from a series of novel dual-functional zwitterionic polymers, Poly[*NRZI*], which were easily obtained via ring-opening metathesis polymerization (ROMP) followed by a single step transformation of the cationic precursor, Poly[*NR(+)*], to the zwitterion, Poly[*NRZI*]. The resulting unique dual-functional structure contained the anion and the cation within the same repeat unit but on separate side chains, enabling the hydrophilicity of the system to be tuned at the repeat unit level. These dual-functional zwitterionic polymers were specifically designed to investigate the impact of structural changes, including the backbone, hydrophilicity, and charge, on the overall nonfouling properties. To evaluate the importance of backbone structure, and as a direct comparison to previously studied methacrylate-based betaines, norbornene-based carbo- and sulfobetaines (Poly[*NCarboZI*] and Poly[*NSulfoZI*]) as well as a methacrylate-based sulfobetaine (Poly[*MASulfoZI*]) were synthesized. These structures contain the anion–cation pairs on the same side chain. Nonfouling coatings were prepared from copolymers, composed of the zwitterionic/cationic precursor monomer and an ethoxysilane-containing monomer. The coatings were evaluated by using protein adsorption studies, which clearly indicated that the overall hydrophilicity has a major influence on the nonfouling character of the materials. The most hydrophilic coating, from the oligoethylene glycol (OEG)-containing dual-functional betaine, Poly[*NOEGZI-co-NSi*], showed the best resistance to nonspecific protein adsorption ($\Gamma_{\text{FIB}} = 0.039 \text{ ng/mm}^2$). Both norbornene-based polymers systems, Poly[*NSulfoZI*] and Poly[*NCarboZI*], were more hydrophilic and thus more resistant to protein adsorption than the methacrylate-based Poly[*MASulfoZI*]. Comparing the protein resistance of the dual-functional zwitterionic coatings, Poly[*NRZI-co-NSi*], to that of their cationic counterparts, Poly[*NR(+)-co-NSi*], revealed the importance of screening electrostatic interactions. The adsorption of negatively charged proteins on zwitterionic coatings was significantly less, despite the fact that both coatings had similar wetting properties. These results demonstrate that the unique, tunable dual-functional zwitterionic polymers reported here can be used to make coatings that are highly efficient at resisting protein adsorption.



INTRODUCTION

Biofouling, or biofilm formation, remains a challenging problem for numerous fields ranging from biomedical applications¹ and marine coating technologies² to water purification, transport, and storage systems.³ Undesirable consequences of this ubiquitous problem include, but are not limited to, reduction in the efficacy/sensitivity of devices, operational losses, thrombosis, and microbial infections.⁴ In the U.S. alone, about half of the 2 million cases of hospital acquired infections are associated with bacterial biofilm formation on biomedical devices such as catheters, surgical implants, and prosthetics. In addition to causing various severe or fatal health complications, such infections place a significant economic burden on society. Estimated direct costs associated with these hospital-acquired infections exceed \$3 billion annually.⁵ Similarly, biofouling on ship hulls, caused by the buildup of marine microorganisms, plants, algae, and crustaceans, can reduce vessel speed by up to 10%, resulting

in a 40% increase in fuel consumption to counteract the added drag. Increased fuel costs combined with the cost of additional maintenance translates to roughly an extra \$500 million annually.⁶ Therefore, development of new technologies and materials that reduce or completely prevent any undesired deposition of microorganisms is of great importance. However, tailoring an efficient nonfouling material requires understanding the interactions involved, which is hindered by the complexity of the process, making it challenging to provide solutions to the problem.

Biofilm formation generally starts within seconds following implantation of a given material (e.g., medical implant) in body fluids, such as blood. The first step of the process is the adsorption of proteins on the substrate surface, which is followed by a cascade

Received: September 20, 2011

Revised: November 22, 2011

Published: November 29, 2011

of larger, more complex species that include microorganisms such as bacteria, fungi, and algae.⁷ Thus, one can argue that the larger microorganisms rarely interact with the clean surface but rather with the proteins adsorbed on it.⁸ At the interface of materials science and biology, several different approaches have been employed to prevent the biofouling process. One approach is to incorporate antimicrobially active ingredients such as antibiotics, biocidal molecules, and silver particles in the material, by blending them with the plastic of the device, covalently attaching them, or coating/painting them onto the material.^{5,9} However, for this approach, once a certain amount of cell debris has formed, the surface activity decreases as the active material can no longer reach the pathogen. An alternative approach is to prevent biofouling by impeding the attachment of a broad range of species rather than killing them. Since the first step of biofouling is protein adsorption, efforts focused on preventing their initial adhesion to the substrate, which would significantly reduce the subsequent adhesion of other species, would appear to provide a longer-standing solution to the problem.¹⁰ The challenge of this approach is that even 0.1 ng/mm² of protein adsorption on a surface can induce full scale biofilm formation, resulting in loss of function of the implantable device.¹¹

Despite the amount of research done in the area, there are few materials that can effectively fulfill this requirement and resist biofilm formation. To date, the most widely employed protein-resistant materials are based on poly(ethylene glycol) (PEG) or oligo(ethylene glycol) (OEG).¹² While the exact mechanism of action of these materials is still debated, the promising results led to extensive efforts in developing new methods to immobilize PEG on surfaces, including physisorption,^{13,14} chemisorption,^{12,15} and covalent grafting.^{16–18} Even though OEG self-assembled monolayers (SAMs) exhibited low protein adsorption values (0.3–3 ng/mm²),¹⁹ their propensity for defects and limited use on metal surfaces led to the development of OEG/PEG coatings via surface-initiated polymerization.^{20,21} This technique produced thicker, more densely packed, robust coatings composed of PEG brushes which reduced protein adsorption values to as low as 0.1 ng/mm².¹⁶ PEG shows effective nonfouling character; however, it is unstable in the presence of oxygen and transition metal ions, resulting in loss of function in most biological media.²² As a result, there is still an ongoing search for alternative, more robust materials that successfully resist protein adsorption. Whitesides and co-workers^{10,23,24} designed and analyzed a series of SAMs containing different functional groups leading to the important observation that the best functional groups for inhibiting protein adsorption shared several common features: the presence of hydrophilic groups, hydrogen-bond donors, and electrical neutrality.

This insight has been used in the design strategy of future nonfouling materials. Among them, zwitterionic polymers, having a highly hygroscopic nature similar to PEG, as well as lipid-like biomimetic features (e.g., 2-methacryloyloxyethylphosphorylcholine (MPC)-based macromolecules),^{25–30} were shown to be promising protein-resistant materials. MPC-based coatings gave protein adsorption amounts varying from 0.03 ng/mm² (brushes prepared via grafting from)³¹ to 3 ng/mm² (bulk coatings).³² These materials showed suppression of clot formation and platelet adhesion, even when in contact with human whole blood without anticoagulants.³⁰ In addition to the MPC-based materials, other zwitterionic structures that have been investigated include carboxybetaines, sulfobetaines, and surfaces prepared from a 1:1 mixture of cationic and anionic SAMs or

monomers.^{10,33–35} The first example of sulfobetaine-based low-fouling coatings was reported by Lowe et al.³⁶ The biofouling resistance of these coatings was tested against bacteria, macrophage, and fibroblast cells, and the bioadhesion was found to be considerably lower than that of the poly(methyl methacrylate) control coatings. Similar surfaces were prepared by Jiang and co-workers through surface-initiated atom transfer radical polymerization (ATRP) and had more controlled and densely packed chains.^{37,38} These surfaces, composed of zwitterionic brushes, had a higher packing density and showed better resistance to protein adsorption (0.003–0.01 ng/mm²) than zwitterionic SAMs (0.01–0.1 ng/mm²).³⁹ Even though these studies indicate that zwitterionic systems show comparable, or in some cases, even better protein resistance than PEG-based materials, they are still prone to failure in long-term usage.^{29,40} Methacrylate-based MPC, sulfo-, and carboxybetaines are all composed of ester linkages, making them hydrolyzable under physiological conditions. In addition, they suffer from complex or labor-intensive coating preparation conditions, including requirements for air- and moisture-free media during the preparation process. Regardless of the intended application, there is still a need for more stable and effective structures as well as efficient ways of incorporating them into coatings.

In this report, we introduce novel zwitterionic molecules based on ring-opening metathesis polymerization (ROMP) as foundational materials for nonfouling coatings. Two polymer systems, shown in Figure 1a,1b, were designed and synthesized. The first system is composed of a series of polymers that carry dual functionality at the repeat unit level (Figure 1a), consisting of a zwitterionic functionality coupled with an alkyl moiety that is systematically tuned to adjust the relative hydrophilicity/phobicity of the overall system, using oligoethylene, methyl, and octyl chains. To the best of our knowledge, this is the first example of such a system, and it is easily obtained using the ROMP chemistry platform. The second system, shown in Figure 1b, is established as a direct comparison to the previously well-studied methacrylate (MA)-based betaines (Figure 1c) to provide insight into whether the methacrylate backbone, in addition to the betaine functionality, is critical for achieving the reported nonfouling properties. Using these zwitterionic polymers as the base for nonfouling coatings, we investigated how structural changes of the zwitterionic material, including the hydrophilicity/phobicity and backbone, impacted their overall nonfouling properties against several proteins including albumin, fibrinogen, and lysozyme.

RESULTS AND DISCUSSION

Polymer Synthesis and Characterization. A summary of all the monomers and the strategies used to synthesize them are shown in Scheme 1. Even though ring-opening metathesis polymerization (ROMP) can be successfully utilized to synthesize well-defined ionic polymers,^{41–45} it is also well-known that the reaction kinetics can be significantly retarded or stopped in the presence of particular functionalities, such as amine, carboxylate, and hydroxyl groups.^{46–49} Therefore, to prevent the carboxylate group of the zwitterionic monomers from diminishing the polymerization kinetics, monomers **2a–2d** were synthesized as quaternary ammonium (cationic) precursors. The monomer **2e**, NSulfoZI (for nomenclature see Figure 1 caption), was obtained in its zwitterionic form, as the sulfonate functionality has been shown not to interfere with ROMP kinetics.^{43,45}

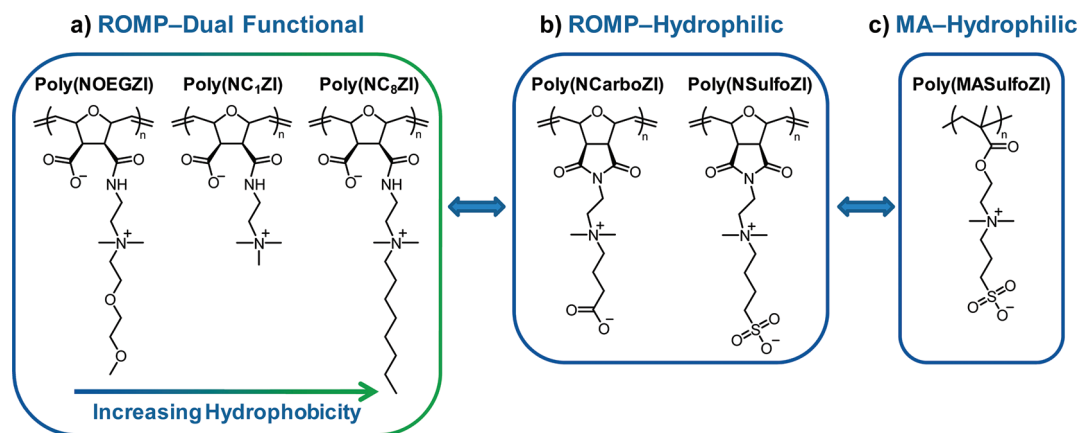
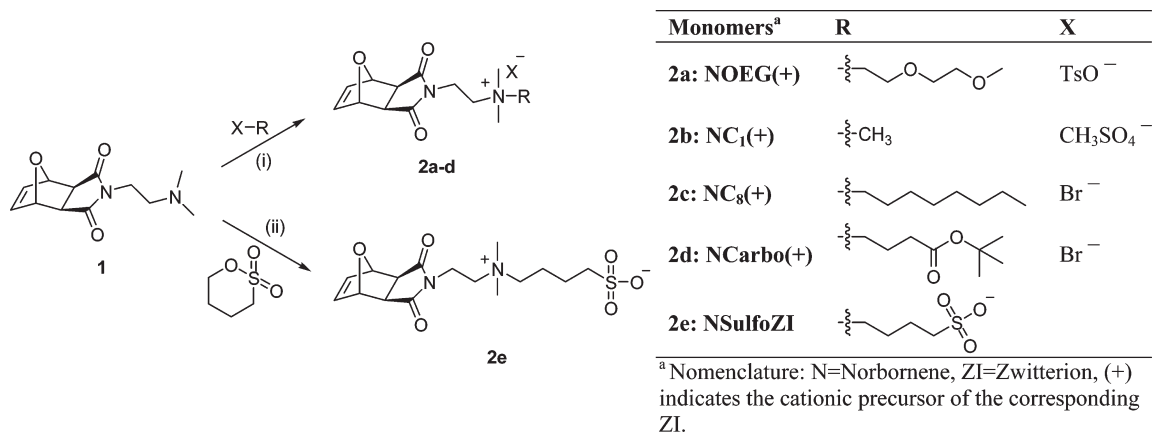


Figure 1. Summary of synthesized zwitterionic polymers and their design principles. (a) ROMP-based, dual-functional betaines with tunable hydrophilicity/phobicity, (b) ROMP-based carboxy- and sulfobetaines, and (c) MA-based sulfobetaine. N = norbornene, ZI = zwitterion, MA = methacrylate, OEG = oligoethylene glycol, C₁ = methyl, and C₈ = octyl.

Scheme 1. Monomer Synthesis^a



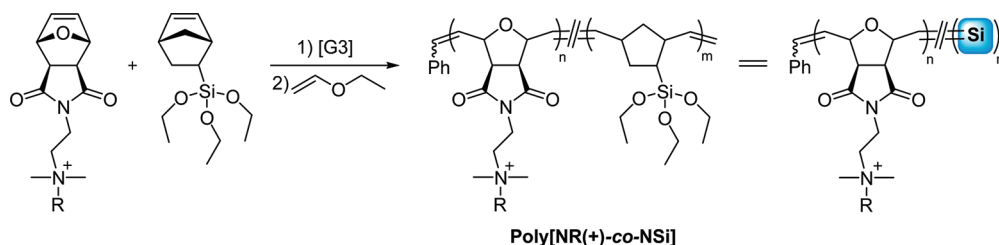
^a Conditions and reagents: (i) **2a**: THF, 50 °C, 48 h; **2b**: THF, 0 °C, 48 h; **2c**: THF, 50 °C, 48 h; **2d**: THF, 50 °C, 48 h. (ii) 1,3-Dinitrobenzene (1 wt %), acetonitrile, 50 °C, 48 h.

The quaternization of the tertiary amine precursor, **1**, was done through its alkylation with an OEG, a methyl, octyl, or *tert*-butyl butyrate chain bearing a good leaving group (TsO⁻, CH₃SO₄⁻, or Br⁻) (see Table in Scheme 1 and see Supporting Information for detailed synthetic procedures). For **2a–2c**, the alkyl chains were selected to systematically increase the hydrophobicity of the targeted zwitterionic functionality.

Ionic polymers are intrinsically hydrophilic, making them soluble in aqueous environments. Therefore, to form stable coatings, the polymers must be covalently attached to the substrate to prevent their dissolution into the surrounding media, which would eventually result in loss of surface activity. Although attaching these ROMP-based polymers to solid surfaces is nontrivial, it is essential to their development as coating materials. Attachment of previously studied nonfouling polymers required complex and highly sophisticated immobilization methods or grafting brushes to/from surfaces which are not suitable for larger-scale applications.^{16,37,50} In order to prepare coatings that can be easily applied on a large scale at ambient conditions, all of the monomers were copolymerized in a random fashion with an ethoxysilane-containing monomer, 5-bicycloheptenyl triethoxysilane (NSi) (Scheme 2). The ethoxysilane

units on the resulting copolymer chains were used to both covalently attach them to the silica/glass surface, through the formation of strong Si–O–Si bonds, and to improve the stability of the coatings through interchain cross-linking.^{50,51}

All the monomers were copolymerized in a mixture of dichloromethane (DCM) and 2,2,2-trifluoroethanol (TFE) to provide a homogeneous medium for the polymerization, where DCM was selected as a good solvent for the catalyst and 5-bicycloheptenyltriethoxysilane, and TFE for the ionic monomers.^{45,52} The third-generation Grubbs' catalyst was used as the initiator for all of the polymerizations and they were terminated using ethyl vinyl ether as the quencher (Scheme 2). ¹H NMR analysis was used to investigate the extent of polymerization, where the complete disappearance of the peaks at 6.50 and 5.15 ppm, corresponding to the double bond protons of the norbornene ring, and the appearance of broad peaks around 6.15 and 5.90 ppm, corresponding to the unsaturated protons of the backbone, indicated complete conversion (see Supporting Information). The copolymer compositions were adjusted to contain 15–20 mol % of the ethoxysilane-containing monomer so that a sufficient

Scheme 2. Copolymer Synthesis^a

^a Nomenclature: Poly[NR(+)-co-NSi], N = norbornene backbone, R = alkyl group, and NSi = 5-bicycloheptenyl triethoxysilane. All the copolymers were synthesized with $n = 30$ and $m = 6$ as the degree of polymerization values of the corresponding monomers to yield 16.6% Si per polymer chain.

quantity of anchoring groups was present for strong adhesion, without compromising the overall hydrophilic character of the coatings.

Along with the copolymers of **2a–2e** and 5-bicycloheptenyl-triethoxysilane, two additional copolymers, Poly[NCH₃-co-NSi] and Poly[MASulfoZI-co-MASi], were synthesized using the same design principles (see Supporting Information for detailed synthetic procedures). These two copolymers were designed to produce control coatings. Poly[NCH₃-co-NSi] was synthesized as the neutral hydrophobic control (structure shown in Supporting Information). Since this polymer contains the identical backbone of the zwitterionic polymers, its performance would provide information about the importance of the zwitterionic functionality in nonfouling behavior. Poly[MASulfoZI-co-MASi], a methacrylate sulfobetaine monomer copolymerized with an ethoxysilane monomer, was prepared using ATRP as a control coating.^{53,54} It is well-known that the nonfouling character of a coating is greatly influenced by the surface composition (i.e., packing density, thickness, architecture) of the active material.⁴ In order to compare the protein resistance of these novel zwitterionic polymers to the well-studied MASulfoZI, it was critical to prepare “identical”, or as similar as possible, surfaces. Therefore, Poly[MASulfoZI-co-MASi] was synthesized in a similar manner to the norbornene-based copolymers to eliminate any factors that could arise due to differences in coating methods and enable a direct comparison to the methacrylate sulfobetaines reported in the literature. Comparing the coatings made from zwitterions with methacrylate and norbornene backbones, Poly[MASulfoZI-co-MASi] and Poly[NSulfoZI-co-NSi], allowed insight as to whether the polymer backbone structure significantly affects protein adsorption.

Gel permeation chromatography (GPC) of charged polymers is challenging due to the likelihood of large aggregate formation or interactions with the stationary phase of the chromatographic column.⁵⁵ It requires specialized columns and an aqueous mobile phase. Additionally, the copolymers synthesized here contain ethoxysilane units that are readily hydrolyzable in aqueous media, facilitating cross-linking reactions and the formation of insoluble material. Thus, the molecular weight characterization of the synthesized polymers was done by end-group analysis using ¹H NMR spectroscopy. Previously, we demonstrated the living ROMP of Poly[NCarboZI] and Poly[NSulfoZI] as well as a direct comparison between ¹H NMR and absolute molecular weight, which showed high correlation.⁴⁵ The molecular weights as well as the molar compositions of the copolymers were determined by comparing the integration values of the phenyl end-group protons to the protons specific to each comonomer. Detailed molecular weight characterization of all the polymers is

Table 1. Molecular Weight Characterization of the Copolymers Synthesized

polymer	theoretical ^a		experimental ^b		
	M_n [kDa]	M_n [kDa]	n^c	m^c	%Si ^e
Poly[NOEG(+)-co-NSi]	16.9	19.7	34.6	8.0	18.8
Poly[NC ₁ (+)-co-NSi]	12.4	9.5	22.5	5.0	18.1
Poly[NC ₉ (+)-co-NSi]	14.3	14.8	30.0	7.5	20.0
Poly[NCarbo(+)-co-NSi]	15.3	11.1	21.0	5.6	21.0
Poly[NSulfoZI-co-NSi]	12.7	n.d. ^d	32.3 ^d	6.0 ^d	15.7
Poly[NCH ₃ -co-NSi]	6.9	7.2	29.4	7.5	20.3
Poly[MASulfoZI-co-MASi]	10.1	9.5	27.9	5.7	16.9

^a Theoretical: $n = 30$, $m = 6$, and %Si = 16.6. ^b M_n , n , m , and %Si determined by end-group analysis of ¹H NMR. ^c See Scheme 2 for n and m . ^d Determined from the ratio of n/m since the end-group was not seen on the ¹H NMR spectra taken in D₂O. ^e %Si = mole percent of 5-bicycloheptenyl triethoxysilane present in the copolymer composition.

shown in Table 1. (For the ¹H NMR spectra, see Supporting Information Figures S4–S10.) The molecular weights and monomer compositions calculated using the degree of polymerization of the corresponding monomers, as determined by ¹H NMR analysis, were in strong agreement with the theoretical ones.

Coating Preparation and Characterization. The copolymerization of the ionic monomers with the ethoxysilane functionality allowed for a very simple coating preparation procedure, which is illustrated in Figure S11. The resulting coatings were durable and resistant to acid and base solutions, which allowed for the postcure functionalization of the cationic coatings to yield their zwitterionic counterparts. Among the cationic precursor coatings, Poly[NCarbo(+)-co-NSi] was subjected to postfunctionalization using acid (4 M HCl/dioxane) to remove the *tert*-butyl group and yield Poly[NCarboZI-co-NSi] (see Scheme in Figure S12), while the remaining ones were treated with dilute base (0.1 M NaOH) to ring open the cyclic maleimide and obtain their zwitterionic counterparts (see Scheme in Figure S13). Poly[NSulfoZI-co-NSi], Poly[MASulfoZI-co-MASi], and Poly[NCH₃-co-NSi] required no further treatment as they were polymerized in their zwitterionic or final functional forms.

Surface compositions for coatings requiring postfunctionalization were analyzed, before and after treatment, using Fourier transform infrared–attenuated total reflectance spectroscopy (FTIR-ATR) and X-ray photoelectron spectroscopy (XPS). The cationic coatings of the dual-functional system, Poly[NR(+)-co-NSi], were treated with 0.1 M NaOH solution to yield

Table 2. Hydrophilicity Measurements of the Monomers and Zwitterionic Coatings Prepared

polymer	R_t (min) ^a	water contact angle (deg)			roughness (nm) ^b
		θ_{static}	$\theta_{\text{advancing}}$	θ_{receding}	
Poly[NOEGZI-co-NSi]	5.9	32 ± 1	32 ± 2	18 ± 1	0.5
Poly[NC ₁ ZI-co-NSi]	7.3	36 ± 4	38 ± 5	23 ± 3	0.5
Poly[NC ₈ ZI-co-NSi]	30.9	70 ± 3	54 ± 1	31 ± 1	1.3
Poly[NSulfoZI-co-NSi]	6.5	43 ± 2	42 ± 3	25 ± 3	0.4
Poly[NCarboZI-co-NSi]	9.8	49 ± 2	50 ± 4	26 ± 2	0.4
Poly[MASulfoZI-co-MASi]	7.2	63 ± 4	70 ± 1	41 ± 2	0.3

^a Retention times (R_t) of the corresponding monomers as measured by HPLC using a C₈ column with a gradient of 1% CH₃CN/min starting with 100% water. ^b Rms roughness was calculated with the AFM manufacturer's provided software on images of 1 $\mu\text{m} \times 1 \mu\text{m}$ scan size.

their zwitterionic forms, Poly[NRZI-co-NSi]. The cyclic imide functionality of the norbornene monomer, provided that it contains a neighboring quaternary ammonium group, can be easily ring-opened under basic conditions to yield amide and carboxylic acid moieties (see scheme in Figure S13).⁴⁵ This single step transformation, easily obtainable using our ROMP platform, was the key point in the design and synthesis of the dual-functional systems introduced here (Figure 1a). As a result, novel structures that carry a hydrophilic/phobic functionality coupled with the zwitterionic one, in the same repeat unit, were obtained. In comparison to the traditional zwitterionic polymers that have the cation and the anion on the same side chain, these dual-functional zwitterions contained the cationic and the anionic functionalities on separate side chains, however, still within the same repeat unit. Figure S13 shows the FTIR-ATR spectra of a representative coating before and after postfunctionalization, in which the reduction of the peak at 1706 cm^{-1} , corresponding to the imide carbonyl stretching and appearance of new peaks at 1660 and 1587 cm^{-1} , corresponding to amide carbonyl stretching along with a broad peak at 3300 cm^{-1} of N–H stretching, indicated extensive conversion. A small peak remaining at 1706 cm^{-1} was an indication that the bottom of the coating was not fully functionalized. However, we further confirmed that the unreacted material was only at the bottom of the coatings, as full conversion on the coating surface was observed by XPS, where a shift in the nitrogen 1s binding energy from 400 to 398 eV was observed upon conversion from imide to amide (see Supporting Information Figure S14).

The deprotection of the carboxylate of Poly[NCarbo(+)-co-NSi] was performed via acid treatment to yield Poly[NCarboZI-co-NSi] (scheme in Figure S12). Figure S12 shows the FTIR spectra obtained before and after the deprotection step. A decrease in the intensity of the peak that corresponds to both the ester and the imide carbonyl stretching at 1703 cm^{-1} was observed due to the conversion of the ester to an acid, while the imide stayed intact. The appearance of two new peaks at 1665 and 1578 cm^{-1} , both corresponding to the carboxylate carbonyl stretching, indicated a successful transformation. This ring-opening reaction and the removal of the *tert*-butyl group were previously reported for similar structures in solution.⁴⁵ Both ¹H NMR and FTIR indicated that those reactions proceeded quantitatively to generate the desired zwitterions.⁴⁵

Coating thickness was easily tuned by varying the polymer concentration of the spin-coating solution (see Supporting Information Figure S16). However, to be consistent throughout all the studies, coatings were prepared from 1% w/v polymer solutions. The resulting coating thicknesses were measured using

single wavelength ellipsometry and ranged from 20 to 35 nm. These results were in agreement with the measurements obtained from atomic force microscopy (AFM) using section analysis (Figure S17). The surface morphology of these coatings, analyzed by AFM, was found to be relatively smooth with no phase separation and roughness ranging from 0.5 to 1.3 nm (see Table 2 and Figure S18). AFM also revealed only minor swelling (2–3 nm) of the films upon immersion in water, indicating highly cross-linked network formation.

Contact angle measurements using the sessile drop method were performed to analyze the hydrophilicity of the coatings. The results are summarized in Table 2. Poly[NOEGZI-co-NSi] had the lowest contact angle, $\theta_{\text{static}} = 32^\circ \pm 1^\circ$ ($\theta_{\text{A}}/\theta_{\text{R}} = 32^\circ/18^\circ$), indicating that this was the most hydrophilic coating obtained. Within the dual-functional series (Figure 1a), increasing contact angle values were observed with increasing hydrophobicity of the alkyl chain, with Poly[NC₈ZI-co-NSi] being the most hydrophobic coating ($\theta_{\text{A}}/\theta_{\text{R}} = 54^\circ/31^\circ$). These results were in agreement with HPLC retention times (R_t) of the corresponding zwitterionic monomers (Table 2). The contact angle values for Poly[NCarboZI-co-NSi] and Poly[NSulfoZI-co-NSi] were within the same range, while Poly[MASulfoZI-co-MASi] demonstrated a relatively higher contact angle. HPLC results also tracked with contact angles for these monomers; however, HPLC and contact angle values did not track across zwitterionic type. For example, Poly[NC₁ZI-co-NSi] has $\theta_{\text{A}}/\theta_{\text{R}} = 38^\circ/23^\circ$ and a 7.3 min R_t of its corresponding monomer (NC₁ZI); however, while MASulfoZI has a very similar R_t of 7.2 min, its corresponding coating, Poly[MASulfoZI-co-MASi], has higher contact angles ($\theta_{\text{A}}/\theta_{\text{R}} = 70^\circ/41^\circ$) (Table 2). Overall, it can be clearly seen that within the dual system the wettability of the coatings is strongly influenced by the hydrophilicity of the side chains, which was in accordance with expectations. The contact angle values of the cationic precursors showed similar wetting properties to their zwitterionic counterparts (Table S1). The comparison of the cationic precursors to their zwitterionic forms, having the same molecular composition and thus similar wetting properties, but different ionic characters, allowed the effect of charge on the nonfouling character of a coating to be examined.

Protein Adsorption Studies. Preventing, or at least minimizing, the adsorption of proteins is believed to be the key point in providing longer-lasting solutions to the biofouling problem.⁴ Therefore, evaluating the ability of these coatings to resist nonspecific protein adsorption was studied using five different proteins (Table S2). These particular proteins were chosen in order to investigate two factors. First, to test the efficacy of the

Table 3. Protein Adsorption Amounts on the Zwitterionic Coatings and the Controls, As Obtained from Ellipsometry Measurements

polymer	protein adsorption amount (ng/mm ²)				
	BSA	fibrinogen	lysozyme	myoglobin	cytochrome c
Poly[NOEGZI-co-NSi]	0.046 ± 0.01	0.04 ± 0.02	0.65 ± 0.11	0.24 ± 0.06	0.41 ± 0.08
Poly[NC ₁ ZI-co-NSi]	0.49 ± 0.06	0.76 ± 0.22	0.70 ± 0.15	0.45 ± 0.13	0.26 ± 0.07
Poly[NC ₈ ZI-co-NSi]	4.79 ± 1.04	3.44 ± 0.24	3.51 ± 0.58	1.63 ± 0.10	1.30 ± 0.04
Poly[NSulfoZI-co-NSi]	0.12 ± 0.08	1.03 ± 0.23	0.96 ± 0.16	0.63 ± 0.04	0.93 ± 0.07
Poly[NCarboZI-co-NSi]	0.59 ± 0.06	0.84 ± 0.26	0.56 ± 0.07	0.95 ± 0.10	0.65 ± 0.17
Poly[MASulfoZI-co-MASi]	0.83 ± 0.02	3.39 ± 0.11	1.45 ± 0.27	2.01 ± 0.29	0.94 ± 0.08
Poly[NCH ₃ -co-NSi]	1.07 ± 0.09	4.67 ± 0.40	2.94 ± 0.16	1.04 ± 0.10	2.62 ± 0.11
silica	0.47 ± 0.10	4.15 ± 0.02	1.29 ± 0.10	1.37 ± 0.03	2.02 ± 0.10

synthesized coatings to resist the adsorption of common proteins, including bovine serum albumin (BSA), fibrinogen, and lysozyme. Second, to investigate the role of electrostatics on protein adsorption,⁵⁶ while eliminating the effect of protein size (molecular weight). Although albumin, fibrinogen, and lysozyme span a range of electrophoretic mobilities (zeta potentials) from relatively negative (albumin) to positive (lysozyme), they are quite different in size and shape. Larger proteins are known to provide more hydrophobic and van der Waals interaction contacts, and this was shown to enhance protein adsorption.^{57,58} Therefore, to eliminate these effects, two additional proteins were also studied. These were myoglobin and cytochrome c, with negative and approximately neutral electrophoretic mobilities (zeta potentials), respectively, but molecular weights essentially identical to positive lysozyme. Table S2 summarizes the properties of the proteins, including molecular weight, isoelectric point, density, and electrophoretic mobility values (zeta potential) as measured in phosphate buffered saline (PBS) (pH = 7.4).

Prior to protein adsorption, all the surfaces were extensively soaked with PBS to extract any unreacted material. Thickness measurements on these coatings, before and after, showed no significant change, indicating successful cross-linking and strong adhesion to the substrate. A literature procedure^{19,59} was followed for the protein adsorption studies, where the coatings were first hydrated in PBS and then incubated in the protein solutions for 2 h (see Supporting Information for details). These coatings were removed and further washed with an excess of PBS followed by deionized water to remove any loosely adhered proteins, and dried under vacuum prior to any analysis. Protein adsorption on the coatings was studied using two different techniques. Ellipsometry measurements^{60–62} were performed to quantify the amount of adsorbed protein and fluorescence microscopy^{63,64} was employed for qualitative analysis, using fluorescein isothiocyanate (FITC) labeled BSA to visually study protein adsorption. The differences in coating thickness before and after protein adsorption was measured using ellipsometry to yield the thickness of the adsorbed protein layer. The amount of protein adsorbed was calculated by multiplying the thickness of the adsorbed protein layer by its density.^{57,60} Protein adsorption results obtained by both techniques (fluorescence microscopy and ellipsometry) were consistent with each other. In addition to the zwitterionic coatings, their corresponding cationic precursors were also analyzed using the same techniques. This direct comparison between cationic and zwitterionic coatings was

performed to provide further information about the effect of electrostatic interactions on protein adsorption.

Adsorption Summary. Table 3 provides a complete summary of the amounts of protein adsorbed on the zwitterionic coatings and the controls (clean silica, the hydrophobic uncharged Poly[NCH₃-co-NSi], and Poly[MASulfoZI-co-MASi]). (Protein adsorption on the corresponding cationic precursors can be found in Supporting Information Table S3.) This table shows that regardless of the protein used, all the ROMP-based zwitterionic coatings, except the most hydrophobic one (Poly[NC₈ZI-co-NSi]), performed better in resisting nonspecific protein adsorption than the controls. Among them, Poly[NSulfoZI-co-NSi] and Poly[NOEGZI-co-NSi] showed the best resistance, with adsorption amounts as low as $\Gamma_{\text{BSA}} = 0.12 \text{ ng/mm}^2$ and $\Gamma_{\text{FIB}} = 0.039 \text{ ng/mm}^2$, respectively. A similar trend was observed among both the dual-functional system (Figure 1a) and the more traditional zwitterions in which the amount of protein adsorption increased with increasing hydrophobicity (contact angle). In general, this was common to all the proteins studied independent of their physical characteristics. Figure 2 shows the adsorption of fibrinogen on all of the zwitterionic coatings and controls. This protein was selected to simplify the discussion as it emphasizes the trends found among all the zwitterionic coatings summarized in Table 3. In addition, fibrinogen has been widely studied allowing stronger comparisons between these coatings and other surfaces in the literature.^{21,67–69}

Figure 2 shows that, within the dual-functional coating system, as the length of the alkyl chain, or hydrophobicity, was increased, the protein adsorption values increased (Figure 2, dual-functional). While this is the first example of tuning the hydrophilicity of a zwitterionic system at the repeat unit level, similar studies were performed for OEG-based SAMs, where the hydrophilicity of the system was tuned either by modifying the end groups⁶⁵ or by varying the length of the SAMs.^{66,67} Our observations were consistent with the conclusions drawn from these previous studies; lower protein adsorption values were obtained on coatings with higher hydrophilicity. Among the dual-functional coatings, Poly[NOEGZI-co-NSi] showed the lowest fibrinogen adsorption, $\Gamma_{\text{FIB}} = 0.039 \text{ ng/mm}^2$, which was also below the 0.1 ng/mm^2 limit.¹¹ This compares well to the “best performing” surfaces in the literature including surfaces composed of OEG-SAMs⁶⁸ and MASulfoZI-brushes³⁹ that showed fibrinogen adsorption of 0.18 and $<0.02 \text{ ng/mm}^2$, respectively. The Poly[NC₁ZI-co-NSi] coating also performed better than the three controls including the one containing

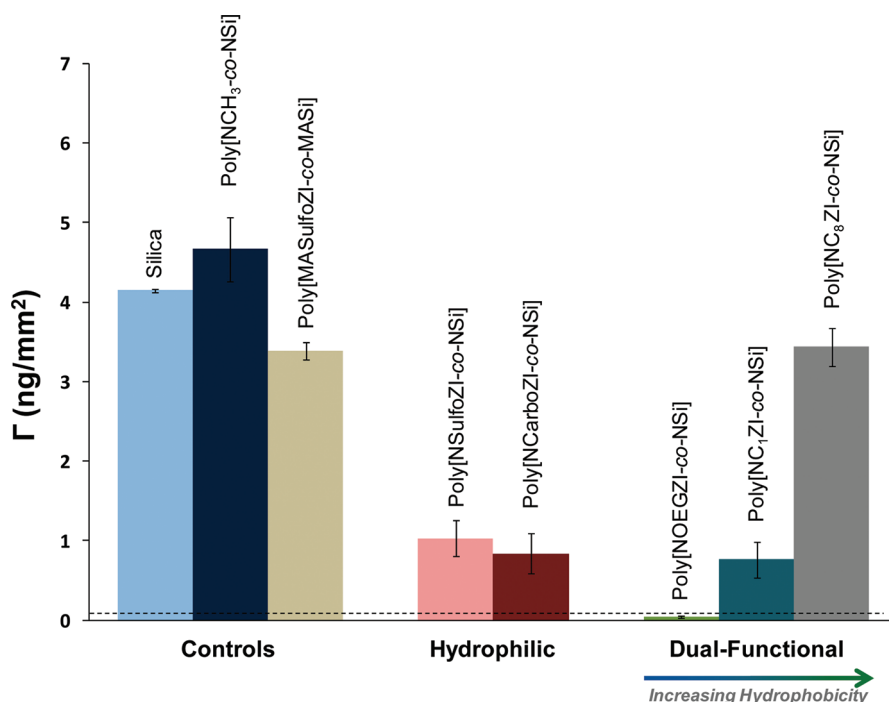


Figure 2. Fibrinogen adsorption on controls and zwitterionic coatings. Dotted line indicates the 0.1 ng/mm^2 protein adsorption limit that can induce full scale biofilm formation, resulting in loss of function of the implantable device.¹¹ Error bars represent standard error from three independent measurements. Data for BSA and lysozyme adsorption are shown in Figures S19 and S20, respectively.

MASulfoZI, which is known to be highly resistant to protein adsorption in polymer brushes.³⁹

For the coatings containing the more traditional zwitterionic groups, protein adsorption also increased with hydrophobicity (contact angle). As shown in Figure 2, both norbornene-based betaines, Poly[NSulfoZI-co-NSi] ($\Gamma_{\text{FIB}} = 1.026 \text{ ng/mm}^2$) and Poly[NCarboZI-co-NSi] ($\Gamma_{\text{FIB}} = 0.84 \text{ ng/mm}^2$), performed better than the three controls including the methacrylate-based sulfobetaine, Poly[MASulfoZI-co-MASi] ($\Gamma_{\text{FIB}} = 3.39 \text{ ng/mm}^2$). Both Poly[NSulfoZI-co-NSi] and Poly[MASulfoZI-co-MASi] contain the same sulfobetaine functional groups and only differ by one methylene group. In methacrylate-based polycarboxylate systems it has been shown previously that when shorter spacers (methylenes) are present between the cationic and anionic group, better resistance to protein adsorption is achieved.⁶⁹ The fact that Poly[NSulfoZI-co-NSi] outperforms Poly[MASulfoZI-co-MASi], given that these coatings are made in a similar fashion and that Poly[NSulfoZI-co-NSi] contains one extra methylene,⁶⁹ indicates that the polymer backbone can positively influence the ability of zwitterionic coatings to resist protein adsorption.

Another important observation also shown in Figure 2 is that Poly[NC₁ZI-co-NSi] and Poly[NCarboZI-co-NSi], composed of the same functional groups (quaternary ammonium as the cation and carboxylate as the anion), showed similar wetting properties and similar protein adsorption amounts ($\Gamma_{\text{FIB}} = 0.76 \text{ ng/mm}^2$ and $\Gamma_{\text{FIB}} = 0.84 \text{ ng/mm}^2$, respectively). However, while Poly[NCarboZI-co-NSi] represents a traditional betaine structure, Poly[NC₁ZI-co-NSi] is quite different (see Figure 1). It contains a trimethylammonium cation and a separate carboxylate anion. The comparison of these two coatings demonstrates that “separation” of the charges in this new architecture does not impair the nonfouling character of the material. This is an important fact

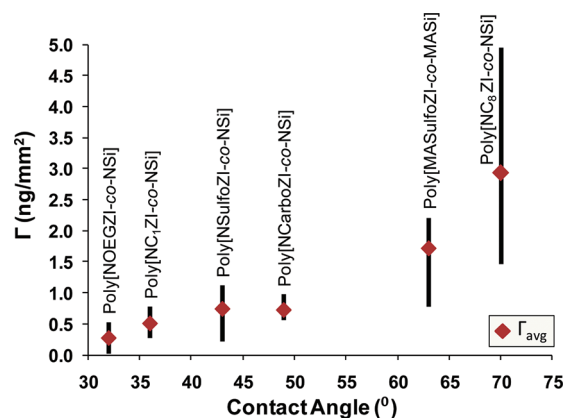


Figure 3. Adsorption vs contact angle for each zwitterionic coating. The diamond symbols represent the average protein adsorption of all five proteins studied. The bars represent the adsorption range observed for all five different proteins (the highest point indicating the highest protein adsorption value observed or vice versa). See Supporting Information Figure S22 for the graph showing all the data points of the corresponding proteins.

because it expands the scope of chemistry one can envisage. As shown here for the first time, this new approach allows the incorporation of various side chains into the zwitterionic functionalities. These moieties can be used to tune the final properties of the zwitterionic materials. The best example of this is Poly[NOEGZI-co-NSi], which showed the strongest resistance to all five proteins studied. The zwitterionic functionality inherently increases the hydrophilicity of the polymer system, which is further improved by the OEG side chain, creating a synergistic effect.

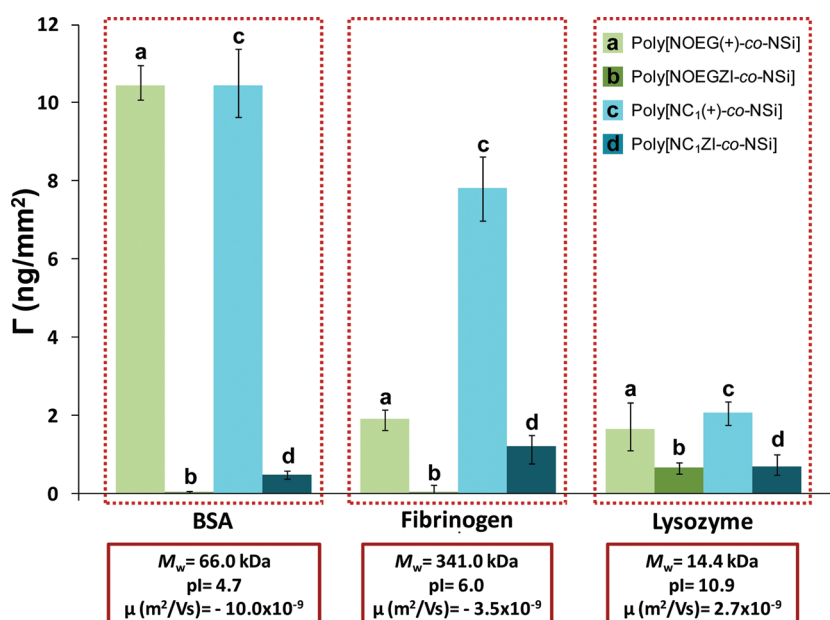


Figure 4. Adsorption behavior of proteins with different isoelectric points and electrophoretic mobilities on cationic and zwitterionic coatings. Error bars represent standard error from three independent measurements. The contact angles for the four samples are $\theta_A/\theta_R = 32^\circ/18^\circ$, $32^\circ/18^\circ$, $38^\circ/21^\circ$, and $38^\circ/23^\circ$ respectively for coatings labeled a, b, c, and d in this figure.

Fluorescence microscopy images of FITC-BSA adsorption on Poly[NSulfoZI-co-NSi] and Poly[MASulfoZI-co-MASi] are shown in Figures S21a and S21b, respectively. These results, which are consistent with the ellipsometry data, indicate that indeed the backbone structure has an important impact on the nonfouling character of the coatings. According to the contact angle measurements (Table 2), it is clear that norbornene-based Poly[NSulfoZI-co-NSi] and Poly[NCarboZI-co-NSi] generate more hydrophilic surfaces than Poly[MASulfoZI-co-MASi], which results in increased wettability of the coatings and thus improved nonfouling character. Figures S21c and S21d compare the fluorescence microscopy images of FITC-BSA adsorption on the cationic coating Poly[NOEG(+)-co-NSi] and its zwitterionic counterpart Poly[NOEGZI-co-NSi]. Both coatings have identical advancing and receding contact angles ($\theta_A/\theta_R = 32^\circ/18^\circ$) yet show remarkably different fluorescent intensities. The fluorescence microscopy image of the cationic coating is much brighter green than the one corresponding to the zwitterionic coating which is again consistent with ellipsometry measurements (also see ellipsometry data discussed below). This suggests that it may be possible to use fluorescence microscopy to screen new coatings for protein adsorption before selecting the “best” ones for quantitative analysis using ellipsometry methods.

Figure 3, which plots protein adsorption as a function of contact angle for all six zwitterionic coatings, also supports the conclusion that backbone structure impacts the nonfouling character of the coating. This graph shows the corresponding average protein adsorption amounts on the specific zwitterionic coatings (red diamonds) as well as the range of the maximum and minimum adsorption observed (the black bars). Figure 3 shows that Poly[NSulfoZI-co-NSi], on average, had lower protein adsorption than Poly[MASulfoZI-co-MASi] and that Poly[NOEGZI-co-NSi] had the lowest average protein adsorption of all the coatings studied. Overall, a clear trend is seen, where the protein adsorption increases with increasing contact angle values, indicating that the greater the

hydrophilicity of a zwitterionic coating, the more efficient it is in resisting nonspecific protein adsorption.

Cationic versus Zwitterionic Coatings. Figures 4 and 5 show protein adsorption for four coatings as a function of protein studied. Figure 4 compares the three widely studied proteins—albumin, fibrinogen, and lysozyme—while Figure 5 compares the three proteins of varying electrophoretic mobility (or zeta potential) but similar size (molecular weight) and shape. From these two figures, three trends are apparent: First, zwitterionic coatings show less protein adsorption than their corresponding cationic coatings despite the fact that they have essentially identical wetting properties (see Figure 4 caption). This result is not necessarily surprising since the importance of electrostatic attraction between surfaces and protein adsorption has been documented; however, the systems described here represent very closely related coatings for making this comparisons.⁵⁶ Second, the amount of adsorbed protein on the cationic coatings tracks with their measured electrophoretic mobilities (zeta potential); as the electrophoretic mobility values of the proteins shifted from more negative to positive, their adsorption decreased. The protein adsorption trend on Poly[NC₁(+)-co-NSi] was $\Gamma_{BSA} > \Gamma_{FIB} > \Gamma_{LYS}$ (Figure 4) and $\Gamma_{MYG} > \Gamma_{CYT-C} > \Gamma_{LYS}$ (Figure 5), while Poly[NOEG(+)-co-NSi] showed a similar trend, but one that was slightly shifted to more negative electrophoretic mobilities, where $\Gamma_{BSA} > \Gamma_{FIB} \sim \Gamma_{LYS}$ (Figure 4) and $\Gamma_{MYG} > \Gamma_{CYT-C} \sim \Gamma_{LYS}$ (Figure 5). This indicates that the cationic OEG containing coatings can limit the adsorption of less negatively charged proteins better than the cationic NC₁ containing coatings. Third, smaller proteins (myoglobin, cytochrome c, and lysozyme) adsorbed more than the larger ones (albumin and fibrinogen) on the zwitterionic coatings, especially on Poly[NOEGZI-co-NSi]. One possible explanation for the observed higher adsorption of the smaller proteins is that these smaller proteins are able to adsorb more effectively onto small defects on the coating surface that are inaccessible to larger proteins. At the same time other explanations, like a higher packing density, yielding higher

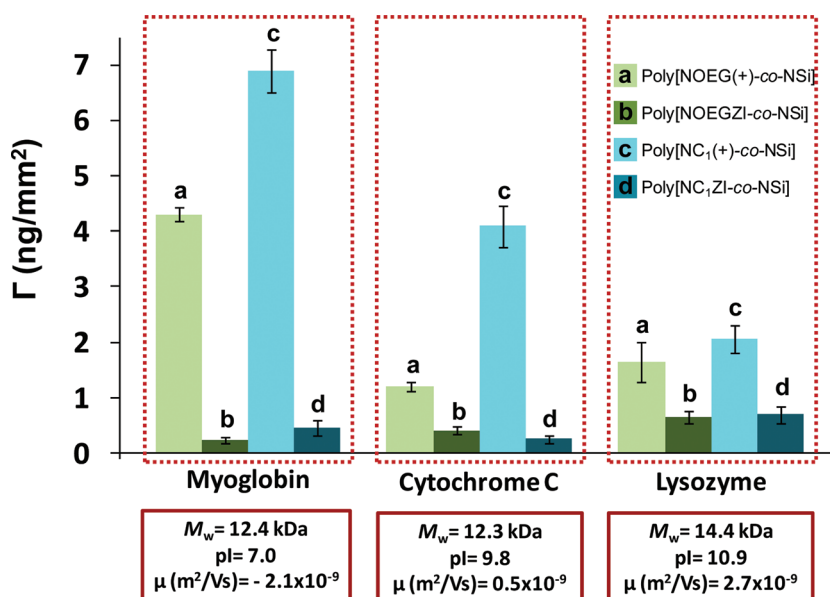


Figure 5. Effect of the protein's electrophoretic mobility (zeta potential) on its adsorption behavior with cationic and zwitterionic coatings. Error bars represent standard error from three independent measurements. The contact angles for the four samples are $\theta_A/\theta_R = 32^\circ/18^\circ$, $32^\circ/18^\circ$, $38^\circ/21^\circ$, and $38^\circ/23^\circ$ respectively for coatings labeled a, b, c, and d in this figure.

adsorption amounts, cannot be ruled out. This observation is in contrast to the expectation that larger proteins can adsorb more due to the increased number of hydrophobic and van der Waals interactions with the surface.⁵⁸

CONCLUSIONS

Novel, norbornene-based zwitterionic polymers were studied as promising materials for nonfouling applications. A novel dual functional system, Poly[NRZI-co-NSi], composed of a hydrophilic/phobic side chain coupled with the zwitterionic functionality, was introduced for the first time. This unique design enabled tuning of the wetting properties of the zwitterionic system by varying the side-chain hydrophobicity at the repeat unit level. In addition, the screening of any electrostatic interactions that might occur between the protein and the coating was shown to be important by the direct comparison of the cationic precursors to their zwitterionic forms, where considerably lower protein adsorption was observed on the zwitterionic coatings.

Poly[NCarboZI-co-NSi] and Poly[NSulfoZI-co-NSi], resembling traditional zwitterionic polymers with the charged groups on the same pendant side chain, were synthesized as a direct comparison to the methacrylate-based sulfobetaine, Poly[MASulfoZI-co-MASi]. This enabled the first direct study on the effect of the backbone structure. Poly[NOEGZI-co-NSi] and Poly[NSulfoZI-co-NSi] outperformed Poly[MASulfoZI-co-MASi] indicating that the methyl methacrylate backbone is not essential and new macromolecular structures can generate better nonfouling materials than these classical zwitterions.

The resistance to protein adsorption of these coatings, investigated by measuring the adsorption amounts of proteins having different physical characteristics, demonstrated the role of improved wettability on imparting nonfouling character to zwitterionic materials. A similar trend was observed within both systems; increased hydrophilicity (lower contact angles) resulted in reduced protein adsorption. The unique dual-functional system has the added advantage of expanding the chemical scope of zwitterions by simply

modifying the side chain. Poly[NOEGZI-co-NSi], the most hydrophilic material, demonstrated the best resistance to non-specific protein adsorption among all the coatings made. Protein adsorption values within the range of previously reported methacrylate-based sulfo- or carbobetaine SAMs (0.01 – 0.1 ng/mm²) and in some cases, significantly lower than the 0.1 ng/mm² limit (amount above which full biofilm formation occurs), were obtained. Poly[NOEGZI-co-NSi], Poly[NC₁ZI-co-NSi], Poly[NCarboZI-co-NSi], and Poly[NSulfoZI-co-NSi] were shown to be promising nonfouling zwitterionic materials easily applicable to large-scale systems. These materials were specifically designed without any hydrolyzable units for improved stability under physiological conditions, making them excellent candidates for applications such as nonfouling coatings, hydrogels, and biological scaffolds.

ASSOCIATED CONTENT

S Supporting Information. All experimental procedures, including monomer and polymer synthesis, as well as detailed information about characterization techniques and protein adsorption studies. This material is available free of charge via the Internet at <http://pubs.acs.org>.

AUTHOR INFORMATION

Corresponding Author

*E-mail: tew@mail.pse.umass.edu.

ACKNOWLEDGMENT

This work was supported by the Office of Naval Research (N00014-10-1-0348) and the National Science Foundation (DMR-0805061, DMR-0820506). Mass spectral data were obtained at the University of Massachusetts Mass Spectrometry Facility, which is supported, in part, by the National Science Foundation. Dr. Ke Zhang is gratefully acknowledged for his

helpful discussion. Authors also thank Ms. Melissa Lackey and Dr. Abhigyan Som for their invaluable comments on early drafts.

REFERENCES

- (1) Werner, C.; Maitz, M. F.; Sperling, C. *J. Mater. Chem.* **2007**, *17*, 3376.
- (2) Krishnan, S.; Weinman, C. J.; Ober, C. K. *J. Mater. Chem.* **2008**, *18*, 3405.
- (3) Flemming, H. C.; Griebe, T.; Schaule, G. In *Antifouling Strategies in Technical Systems - A Short Review*; 18th Biennial Conference of the International-Association-on-Water-Quality; Pergamon-Elsevier Science Ltd.: Dordrecht, 1996; p 517.
- (4) Banerjee, I.; Pangule, R. C.; Kane, R. S. *Adv. Mater.* **2011**, *23*, 690.
- (5) Darouiche, R. O. *New Engl. J. Med.* **2004**, *350*, 1422.
- (6) <http://www.onr.navy.mil/Media-Center/Fact-Sheets/Biofouling-Prevention.aspx> (accessed on May 2011).
- (7) Hall-Stoodley, L.; Costerton, J. W.; Stoodley, P. *Nat. Rev. Microbiol.* **2004**, *2*, 95.
- (8) Knetsch, M. L.W.; Koole, L. H. *Polymer* **2011**, *3*, 340.
- (9) Madkour, A. E.; Dabkowski, J. A.; Nusslein, K.; Tew, G. N. *Langmuir* **2009**, *25*, 1060.
- (10) Kane, R. S.; Deschatelets, P.; Whitesides, G. M. *Langmuir* **2003**, *19*, 2388.
- (11) Tsai, W. B.; Grunkemeier, J. M.; Horbett, T. A. *J. Biomed. Mater. Res.* **1999**, *44*, 130.
- (12) Prime, K. L.; Whitesides, G. M. *J. Am. Chem. Soc.* **1993**, *115*, 10714.
- (13) Elbert, D. L.; Hubbell, J. A. *J. Biomed. Mater. Res.* **1998**, *42*, 55.
- (14) Liu, V. A.; Jastromb, W. E.; Bhatia, S. N. *J. Biomed. Mater. Res.* **2002**, *60*, 126.
- (15) Bearinger, J. P.; Terrettaz, S.; Michel, R.; Tirelli, N.; Vogel, H.; Textor, M.; Hubbell, J. A. *Nature Mater.* **2003**, *2*, 259.
- (16) Hucknall, A.; Rangarajan, S.; Chilkoti, A. *Adv. Mater.* **2009**, *21*, 2441.
- (17) Jo, S.; Park, K. *Biomaterials* **2000**, *21*, 605.
- (18) Malmsten, M.; Emoto, K.; Van Alstine, J. M. *J. Colloid Interface Sci.* **1998**, *202*, 507.
- (19) Sharma, S.; Johnson, R. W.; Desai, T. A. *Langmuir* **2004**, *20*, 348.
- (20) Schonenberger, C.; Sondaghuethorst, J. A. M.; Jorritsma, J.; Fokkink, L. G. J. *Langmuir* **1994**, *10*, 611.
- (21) Ma, H. W.; Wells, M.; Beebe, T. P.; Chilkoti, A. *Adv. Funct. Mater.* **2006**, *16*, 640.
- (22) Shen, M. C.; Martinson, L.; Wagner, M. S.; Castner, D. G.; Ratner, B. D.; Horbett, T. A. *J. Biomater. Sci., Polym. Ed.* **2002**, *13*, 367.
- (23) Chapman, R. G.; Ostuni, E.; Takayama, S.; Holmlin, R. E.; Yan, L.; Whitesides, G. M. *J. Am. Chem. Soc.* **2000**, *122*, 8303.
- (24) Ostuni, E.; Chapman, R. G.; Holmlin, R. E.; Takayama, S.; Whitesides, G. M. *Langmuir* **2001**, *17*, S605.
- (25) Ishihara, K.; Nomura, H.; Mihara, T.; Kurita, K.; Iwasaki, Y.; Nakabayashi, N. *J. Biomed. Mater. Res.* **1998**, *39*, 323–330.
- (26) Ishihara, K.; Aragaki, R.; Ueda, T.; Watanabe, A.; Nakabayashi, N. *J. Biomed. Mater. Res.* **1990**, *24*, 1069.
- (27) Ueda, T.; Watanabe, A.; Ishihara, K.; Nakabayashi, N. *J. Biomater. Sci., Polym. Ed.* **1991**, *3*, 185.
- (28) Ishihara, K.; Ziats, N. P.; Tierney, B. P.; Nakabayashi, N.; Anderson, J. M. *J. Biomed. Mater. Res.* **1991**, *25*, 1397.
- (29) Ueda, T.; Oshida, H.; Kurita, K.; Ishihara, K.; Nakabayashi, N. *Polym. J.* **1992**, *24*, 1259.
- (30) Ishihara, K.; Oshida, H.; Endo, Y.; Ueda, T.; Watanabe, A.; Nakabayashi, N. *J. Biomed. Mater. Res.* **1992**, *26*, 1543.
- (31) Sibarani, J.; Konno, T.; Takai, M.; Ishihara, K. In *Surface Modification by Grafting with Biocompatible 2-Methacryloyloxyethyl Phosphorylcholine for Microfluidic Devices*; Kim, Y. H., Cho, C. S., Kang, I. K., Kim, S. Y., Kwon, O. H., Eds.; ASBM7: Advanced Biomaterials VII; 2007; Vol. 342–343, p 789.
- (32) Xu, Y.; Takai, M.; Konno, T.; Ishihara, K. *Lab Chip* **2007**, *7*, 199.
- (33) Holmlin, R. E.; Chen, X. X.; Chapman, R. G.; Takayama, S.; Whitesides, G. M. *Langmuir* **2001**, *17*, 2841.
- (34) Chen, S. F.; Zheng, J.; Li, L. Y.; Jiang, S. Y. *J. Am. Chem. Soc.* **2005**, *127*, 14473.
- (35) Chen, S.; Jiang, S. *Adv. Mater.* **2008**, *20*, 335.
- (36) Lowe, A. B.; Vamvakaki, M.; Wassall, M. A.; Wong, L.; Billingham, N. C.; Armes, S. P.; Lloyd, A. W. *J. Biomed. Mater. Res.* **2000**, *52*, 88.
- (37) Zhang, Z.; Chao, T.; Chen, S.; Jiang, S. *Langmuir* **2006**, *22*, 10072.
- (38) Zhang, Z.; Chen, S. F.; Jiang, S. Y. *Biomacromolecules* **2006**, *7*, 3311.
- (39) Chang, Y.; Liao, S.; Higuchi, A.; Ruaan, R.; Chu, C.; Chen, W. *Langmuir* **2008**, *24*, 5453.
- (40) Wang, D. A.; Williams, C. G.; Li, Q. A.; Sharma, B.; Elisseff, J. H. *Biomaterials* **2003**, *24*, 3969.
- (41) Ilker, M. F.; Schule, H.; Coughlin, E. B. *Macromolecules* **2004**, *37*, 694.
- (42) Alfred, S. F.; Al-Badri, Z. M.; Madkour, A. E.; Lienkamp, K.; Tew, G. N. *J. Polym. Sci., Polym. Chem.* **2008**, *46*, 2640.
- (43) Rankin, D. A.; Lowe, A. B. *Macromolecules* **2008**, *41*, 614.
- (44) Colak, S.; Nelson, C. F.; Nusslein, K.; Tew, G. N. *Biomacromolecules* **2009**, *10*, 353.
- (45) Colak, S.; Tew, G. N. *Macromolecules* **2008**, *41*, 8436.
- (46) Slugovc, C. *Macromol. Rapid Commun.* **2004**, *25*, 1283.
- (47) Trnka, T. M.; Grubbs, R. H. *Acc. Chem. Res.* **2001**, *34*, 18.
- (48) Lynn, D. M.; Mohr, B.; Grubbs, R. H. *J. Am. Chem. Soc.* **1998**, *120*, 1627.
- (49) Lynn, D. M.; Mohr, B.; Grubbs, R. H.; Henling, L. M.; Day, M. W. *J. Am. Chem. Soc.* **2000**, *122*, 6601.
- (50) Sambhy, V.; Peterson, B. R.; Sen, A. *Langmuir* **2008**, *24*, 7549.
- (51) Colak, S.; Kusefoglu, S. H. *J. Appl. Polym. Sci.* **2007**, *104*, 2244.
- (52) Rankin, D. A.; P'Pool, S. J.; Schanz, H.; Lowe, A. B. *J. Polym. Sci., Polym. Chem.* **2007**, *45*, 2113.
- (53) Dong, H.; Ye, P.; Zhong, M.; Pietrasik, J.; Drumright, R.; Matyjaszewski, K. *Langmuir* **2010**, *26*, 15567.
- (54) Kobayashi, M.; Terada, M.; Terayama, Y.; Kikuchi, M.; Takahara, A. *Macromolecules* **2010**, *43*, 8409.
- (55) Volet, G.; Lesec, J. J. *Liq. Chromatogr.* **1994**, *17*, 559.
- (56) Mueller, B.; Zacharias, M.; Rezwani, K. *Adv. Eng. Mater.* **2010**, *12*, B53.
- (57) Voros, J. *Biophys. J.* **2004**, *87*, 553.
- (58) Jeon, S. I.; Andrade, J. D. *J. Colloid Interface Sci.* **1991**, *142*, 159.
- (59) Sharma, S.; Papat, K. C.; Desai, T. A. *Langmuir* **2002**, *18*, 8728.
- (60) Malmsten, M. *Abstr. Pap. Am. Chem. Soc.* **1994**, *207*, 71.
- (61) Defeijter, J. A.; Benjamins, J.; Veer, F. A. *Biopolymers* **1978**, *17*, 1759.
- (62) Elwing, H. *Biomaterials* **1998**, *19*, 397.
- (63) Kim, J.; Somorjai, G. A. *J. Am. Chem. Soc.* **2003**, *125*, 3150.
- (64) Togashi, D. M.; Ryder, A. G.; Heiss, G. *Colloids Surf., B* **2009**, *72*, 219.
- (65) Herrwerth, S.; Eck, W.; Reinhardt, S.; Grunze, M. *J. Am. Chem. Soc.* **2003**, *125*, 9359.
- (66) Schilp, S.; Rosenhahn, A.; Pettitt, M. E.; Bowen, J.; Callow, M. E.; Callow, J. A.; Grunze, M. *Langmuir* **2009**, *25*, 10077.
- (67) Schilp, S.; Kueller, A.; Rosenhahn, A.; Grunze, M.; Pettitt, M. E.; Callow, M. E.; Callow, J. A. *Biointerphases* **2007**, *2*, 143.
- (68) Li, L.; Chen, S.; Zheng, J.; Ratner, B. D.; Jiang, S. *J. Phys. Chem. B* **2005**, *109*, 2934.
- (69) Zhang, Z.; Vaisocherova, H.; Cheng, G.; Yang, W.; Xue, H.; Jiang, S. *Biomacromolecules* **2009**, *10*, 2686.